



An analysis of heavy metals movements on soils from places with high level risk of flooding and different anthropogenic activities

C. H. Corvalán Moya^{1,2,3*}, C. Bruni^{1,**}, A. Barbini¹, E. Previtali¹

¹Tres de Febrero National University, B1674AHF, Gral. Enrique Mosconi 2750, B1674AHF, Buenos Aires, Argentina

²Atomic National Energy Commission, Avda. Gral. Paz 1499, B1650KNA, Buenos Aires, Argentina

³National Council on Scientific and Technical Research, Buenos Aires, Argentina

*Corresponding author, ccmoya@untref.edu.ar

**Corresponding author, Email address: camilabruni.vz@gmail.com

Received 31 Dec 2023,

Revised 27 Jan 2024,

Accepted 28 Jan 2024

Keywords:

- ✓ Heavy Metals;
- ✓ Mining
- ✓ Flooding
- ✓ Soil pollution;
- ✓ Matter movement;

Citation: Corvalán Moya C., Bruni C., Barbini A. and Previtali E. (2024). An analysis of heavy metals movements on soils from places with high level risk of flooding and different anthropogenic activities, *J. Mater. Environ. Sci.*, 15(1), 162-178

Abstract: Tucumán is located in northwest Argentina. In the south of this province, near the Marapa River, there were many flooding events in the last 30 years.

Heavy metals (HM) constitute an ill-defined group of inorganic chemical hazards, and those most commonly found at contaminated sites are lead (Pb), chromium (Cr), arsenic (As), zinc (Zn), cadmium (Cd), copper (Cu), mercury (Hg), and nickel (Ni). Soils are the major sink for heavy metals released into the environment by anthropogenic activities and their total concentration in soils persists for a long time after their introduction leading to accumulation.

This work presents the soil characterization for heavy metals by ICP technique after made a sampling strategy using satellite imagery. The baseline was determinate without the influence of anthropogenic activities and flooding effects. Then, comparison between this baseline and sampling from flooding zones and principal anthropogenic activities are shown and discussed. Particularly high-level concentrations were found for Cu, Zn and Cr.

1. Introduction

Tucumán is located in northwest Argentina. In the south of this province, near the Marapa River, there were many flooding events in the last 30 years. Previous work showed indicators of contamination by heavy metals in the water of the Marapa River (Butí *et al.*, 2015, Amoroso *et al.*, 1998 and Villegas *et al.*, 2002). Heavy metals (HM) constitute an ill-defined group of inorganic chemical hazards, and those most commonly found at contaminated sites are lead (Pb), chromium (Cr), arsenic (As), zinc (Zn), cadmium (Cd), copper (Cu), mercury (Hg), and nickel (Ni) (Belbachir *et al.*, 2013; Brahimi *et al.*, 2015; and Bazzi *et al.*, 2020). Soils are the major sink for heavy metals released into the environment by anthropogenic activities and unlike organic contaminants which are oxidized by microbial action, most metals do not undergo microbial or chemical degradation, and their total concentration in soils persists for a long time after their introduction leading to accumulation (Jodeh *et al.*, 2015; Yan *et al.*, 2018 and Nyiramigisha *et al.*, 2021).

In this work the baseline determination was made without the influence of anthropogenic activities and flooding effects. Then, comparisons between this baseline and sampling from flooding zones and anthropogenic activities are shown and the potential effects of flooding and industrial activities are discussed.

Floods are known to be “natural disasters” whose origins maybe multifactorial. In physics terms, they could be defined as a chaotic moving phenomenon not only of water but also an advective and diffusive displacement of different elements that could be come pollutants for the region (Owusu *et al.*, 2022; Mazraeh *et al.*, 2023 and Jalili Pirani *et al.*, 2020). These could persist a long time and change the physical-chemical properties of the soil, which is affected by the flood condition described above. In particular, floods that occurred in the south of Tucuman province, acquired some periodicity, showing in the last decades with a progressive frequency (Busnelli, 2009). We propose a soil analysis of possible heavy metals that could have been moved by water as a function of the industrial activity in the region (sugar cane and mining industries). In this way, as a first step it is important to define a comparison patron establishing the baseline, because a wrong comparison patron could lead to an over estimation or under estimation of the concentration values of the analyzed elements.

The study of the soil quality is going to be formed by various investigation steps. According to the Norm IRAM 29481-5, in a first step it is fundamental to find all the possible information about the studied area that allows to know the soil properties and local hydrology. When this step is finished, it is followed by a detailed investigation in which the soil use and every activity done on it is analyzed. Finally, a sampling plan and design is performed, followed by the establishment of a baseline, defined as a state of the studied zone preceding an alteration.

1.1 Description of the studied area

The studied area is located in the Marapa lower basin, between the villages of Graneros and Lamadrid, in the Department of Graneros, Tucuman province, Argentina. The basin belongs to the hydrological system of Salí-Dulce River (Díaz Gómez *et al.*, 2017). The study of this site includes a surface of approximately 230 km², where the zone near the Marapa River is very important (see **Figure 1**). Geographically, the Aconquija Chain is to the west from Pedemonte and depressed flood plain, where the studied area is located which extends towards the east to the Rio Hondo Reservoir.

The predominant soils belong to the orders of Inceptisoils, soils poorly structured, with silt-sand texture and low infiltration. They are succeeded by Molisoils, emerging in the areas with the cattle herding and cultivation of soya, corn, sugarcane and wheat crops. These were created along with deforestation processes (Informe Técnico, 2017).

The native dry forest and pedemountain jungle are estimated to have lost 956 km², between 1983-2017 because of deforestation (Informe Técnico, 2017).

The main urban areas are located only in Graneros, with a population of 2375 inhabitants, and in Lamadrid, with a population of 4580, according to the 2010 census of The National Institute of Statistics and Censuses of Argentina (INDEC).

The Marapa River has a length of 150 km and a hydrographic basin of approximately 900 km². It's origin is in Catamarca, where it extends 10 km towards Tucumán, with the name of Singuil River which leads to the Escaba dam. After the dam, the river is called Marapa and ends in the Rio Hondo Reservoir, Santiago del Estero. It has two main tributaries that contribute with high flows, the San Ignacio River and San Francisco River. There are many streams and old channels between Graneros and Lamadrid that contribute to floodable zones.

The region has a monzonic weather, with a rainy season in summer and a dry season in winter, with an annual average temperature of 17,6 °C (Informe Técnico, 2017). During the summer, intense precipitation can reach levels of 261 mm/day, and the rainiest months are January, February, and March. These intense rains can result in overflows and river floods, which affects nearby villages.

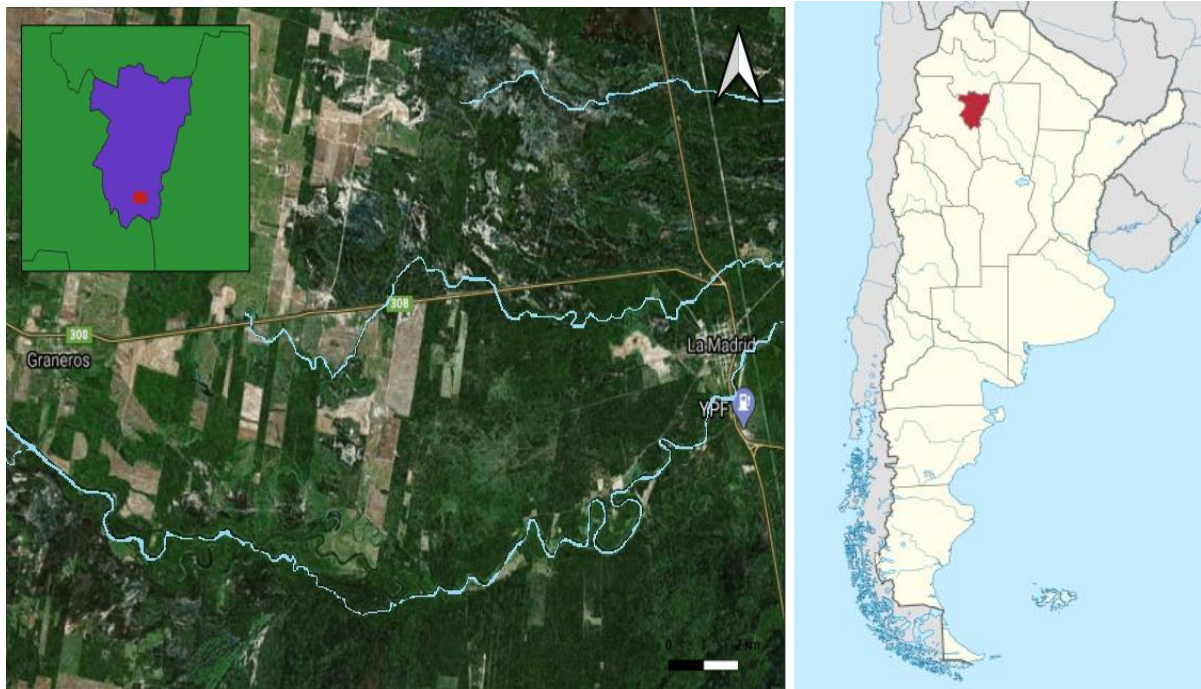


Figure 1. Left side: satellite imagery of the studied zone (taken from Google Earth). The town of Graneros can be seen to the west, and Lamadrid at the east. Right side: Argentina, Tucumán province can be seen to the north

1.2 Background

The flood causes can be multifactorial as discussed above, however, it is important to highlight the high intensity of the precipitations during the summer that cause overflows and floods in the Marapa River and its tributaries. The analysis of precipitation taken from Argentina National Institute of Agricultural Technology (INTA) reports, indicates that the average precipitation until 2015 was 853 mm/year (see Figure 2).

This flooding pattern repeats annually, oscillating, and can coincide with the El Niño phenomenon (Díaz Gómez *et al.*, 2017). However, anthropic development in the region has increased the problem because deforestation, river retours, canalizations and desiccating of Rio Hondo reservoir, together created chaotic conditions of susceptibility to flood (Díaz Gómez *et al.*, 2017). The village of Lamadrid was one of the most affected because of its closeness to Marapa River (see Figure 3). The inhabitants of this village evacuate on their own and take refuge in the north of national road 157, because its ground level is a safe place where the water does not reach.

The anthropic actions that had taken place, such as the extension of the crop borders without planification, associated with extreme weather events caused the increase of filler surface and river flow in the intermediate and low basin. In order to get the scale of the impact of these factors, it is estimated that the harvest surface has increased by 88% between 2001 and 2015. This increase was on the order of 6.000 ha/year, and 40% of Lamadrid surface is used for cattle herding (Recavarren, 2016). The expansion caused a change in the hydrogeomorphological dynamics of the basin, an increase of soil erosion, the sediments transport and the runoff flows. The expansion of the crop area was accompanied by the canalization of the San Francisco River, with it becoming a tributary of the Marapa

River. With this change, the flood volume that was drained to the wet land before, now is added to the Marapa River increasing itsflow. This fact had an important impact in the last floods that took place in Lamadrid.

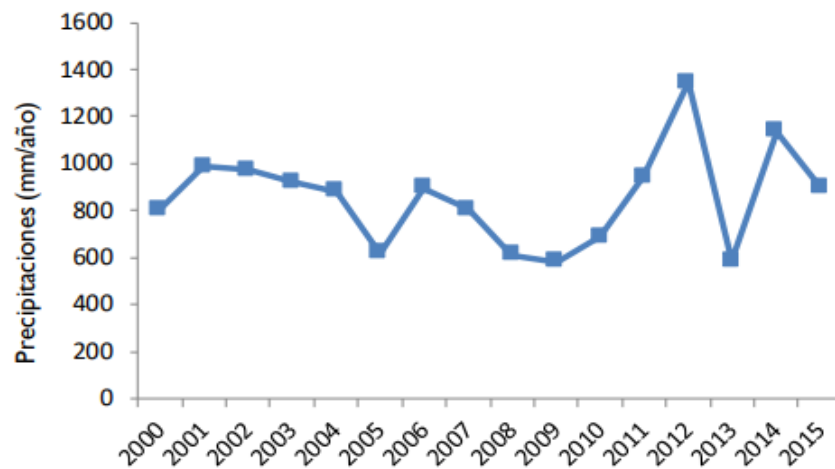


Figure 2. Annual precipitation in General Lamadrid. From the year 2000 to 2015. Source: INTA

Examples of these events are the floods in 2017 and 2019 with catastrophic consequences.



Figure 3. Area of the extension of the flood in 2017. Flood commission report, Tucumán Province (2017) (Informe Técnico, 2017)

2. Methodology

2.1 Sampling strategy

In a first step we considered the importance of establishing a robust baseline for heavy metals on soils in our studied region. Different approaches were used to evaluate the more representative geographical points. The parameters evaluated were flooding and anthropic activities such as sugar cane and mining industries. For this evaluation we used satellite imagery. See Ref. (Barbini *et al.*, 2021) for more details.

2.1.1 Points sampling for the baseline determination and hot points determination

We used many tools for the representative sampling points selection in order to set the baseline. These include a formal and informal bibliography revision (local newspapers), semiquantitative analysis (NDWI, MNDWI index) or SAR imagery (used to compare events in particular dates), and many remote sensing techniques in the platform Google Earth Engine and QGIS. Finally, a ponderation matrix was done with the variables of interest.

Satellite imagery analysis

Of the many space missions for Earth remote sensing, the missions that have been used in this project are Sentinel 1 and Sentinel 2.

Sentinel 1 is a mission that belongs to the Copernicus space program developed by the European Space Agency (ESA). It has two polar-orbit satellites with Synthetic Aperture Radar (SAR). The SAR technology allows researchers to work with bands that cannot be blocked by the clouds and can therefore operate in every weather condition. The products have a resolution from 5 to 20 m per pixel and a sweep width of 400 km. The main applications of these products are oriented at natural disaster management such as floods, landslides, glacier monitoring, etc.

Sentinel 2 also belongs to the ESA Copernicus program. It consists of 2 satellites with a multispectral sensor which includes 13 high-resolution bands with a resolution of 10 to 60 m per pixel. The band combinations provide information about the vegetation, moisture, and flooded zones. This is why the mission is used with crop-oriented purposes, forest monitoring, soil surface change detection, etc. (ESA 2015). The spectral response of a land area is a consequence of the type of surface. The objective of remote sensing is to determine relation between the objects and variables of the land surface with their spectral response, so then it is possible to characterize them. One of the main methods used in remote sensing is combining various bands using operations, resulting in an indicator of a particular kind of surface. These operations are called “indexes”.

We selected the following two indexes for the flooded areas analysis, and performed a comparison of both.

- *NDWI (Normalized Difference Water Index)*

(McFeeters, 1996) proposed the index NDWI defined by the equation:

$$NDWI = (GREEN - NIR) / (GREEN + NIR) \quad (1)$$

It maximizes the water reflectance using the green band, minimizes the NIR (NearInfraRed) low reflectance because of the water properties, and takes advantage of the NIR high reflectance in the vegetation and soil. In consequence, soil and vegetation take negative values and water has positive values (McFeeters, 1996).

- *MNDWI (Modified Normalized Difference Water Index) - (Xu, 2006)*

Xu proposed the use of the NDWI but replacing the NIR band with the MIR band (Middle InfraRed). The equation is:

$$MNDWI = (GREEN - MIR) / (GREEN + MIR) \quad (2)$$

These results in a better water delimitation, suppressing the background noise that some soils and vegetation could cause.

- *SAR Imagery*

The SAR images were acquired from the ESA Sentinel 1 mission. The processing of these images was done in Google Earth Engine, with algorithm applications; it was possible to discriminate the potentially flooded zones. The polarization used was VH (Vertical – Horizontal) recommended by (Hussin, 1995 and Leckie *et al.*, 1998), because it was possible to get better radar reflections in the corners, especially in areas with urban structures (Liao *et al.*, 2020).

With the information acquired from the satellite imagery, the sampling points are proposed. The selection considers particularly four variables: easy access the sampling zone (rural roads), height of the ground level (taken from Digital Elevation Models), distance from water bodies or flooded zones (index analysis from the satellite imagery), anthropogenic alteration (deforestation analysis) in the region and industrial identifications. These variables will be evaluated through a ponderation matrix.

2.2 Sample preparations for experimental characterizations

In order to avoid measurement artifacts, particularly from different soil texture and organic matter, all the samples were prepared before ICP measurements. The samples were taken at each geographical point, three samples by point at different depths, from the surface to 30 cm in depth. Finally the ICP compositional measurements at each point are an average over the depths. The samples labeled from each point were mixed and ground, then sieved to unify the granulometry. To avoid effects of organic matter, a heat treatment (80C-24hr) was performed in a muffle furnace at atmospheric conditions; this was preceded by storing the samples in glass containers.

3. Results and Discussion

3.1 Environmental soil baseline determination

After analyzing and processing the satellite imagery of the flood events in 2017 and 2019, the following results were obtained:

Indexes

In the NDWI and MNDWI results, a mask was applied to discriminate the values greater than 0 (flooded zones). The main affected zones (in white, see [Figure 4](#)) are located in the south of Lamadrid, near the river, and where the San Francisco and Marapa rivers converge, affected and area of 3.7 km². This approximation is a result of a difference between water bodies before the flood (14/03/19) and after the event (03/04/19). After applying the mask to show values greater than 0, the MNDWI showed more area than NDWI. The images selected were clouds free to avoid shadows that could interfere with the results.

The results of the analysis according to each author had some differences. The McFeeters NDWI underestimated widely the flooded areas compared to Xu MNDWI, which showed a more extensive area of potentially flooded zones (Xu, 2006). This difference can be a result of the great amount of sediments dragged by the river, because the NIR band fails if there are sediments in water, or emergent vegetation. Besides, because of the lack of spectral profile of “development zones” (Leckie, 1998), many materials could throw false positives in NDWI and MNDWI, as some of them were detected in Lamadrid urban zones, in the McFeeters NDWI during the flood. On the other hand, the MNDWI index showed more coherent results with respect to the observed satellite imagery. However, there were no zones detected that were known to be flooded inside the Lamadrid village.

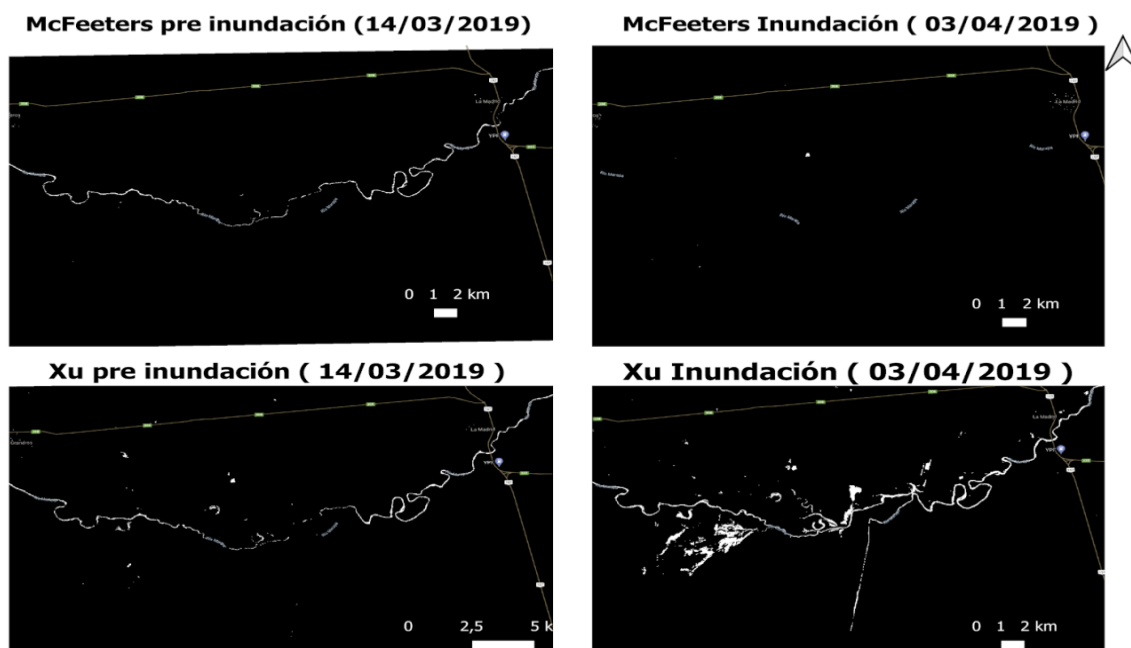


Figure 4. Comparative picture of Marapa river with a mask (white is water), in a region between Graneros and Lamadrid. The NDWI (McFeeters, 1996) and MNDWI (Xu, 2006), applied with values greater than 0.

Ground level and accessibility analysis

A general hydraulic gradient for the Marapa river flow is from northwest to southeast direction. A topographic map shows that the maximum ground level in the zone is located in Graneros between 328 and 320 m.a.s.l., while the minimum ground level is located in Lamadrid between 295 and 283 m.a.s.l. With this aspect, the area in Graneros is less likely to suffer a flood because the surface runoff tends to move to zones with less hydraulic gradients Lamadrid. The urban area has a high vulnerability because its location is in an outletcone of three great basins or discharge areas to the main way of drainage of the system Marapa-Graneros (Informe Tecnico, 2017). Consequently, the area in Lamadrid is not selected for the baseline establishment, but it will be used for the hotspot localizations. The areas north and north-east of Lamadrid were also considered, at the intersection of the national road 157 and provincial road 308, but they were rejected because of the presence of streams and channels that could have historical floods in the zone.

The highest ground level in Graneros is located near the provincial road 308. This characteristic makes the zone an ideal baseline for the study, because of its closeness with the road, making it easy to access and take samples. This is backed by the satellite imagery afforded by the technology of NDWI indexes and SAR imagery, that showed the areas of interest that were not flooded during the vents in 2017 and 2019.

Deforestation and anthropic activity analysis

A map of crop land expansion in the region was done and studied by QGIS (geographic information system software) with the information of Global Forest Watch platform, between the years 2000 and 2019. Figure 5 shows the forest loss to anthropic activities, represented in colors with an interval of four years. The zones with highest anthropic intervention are the most propense to flood because of soil erosion, sediments dragging and runoff flows. The true colors in the picture represent non-altered zones, or zones altered before the twenty-year span covered by our analysis.

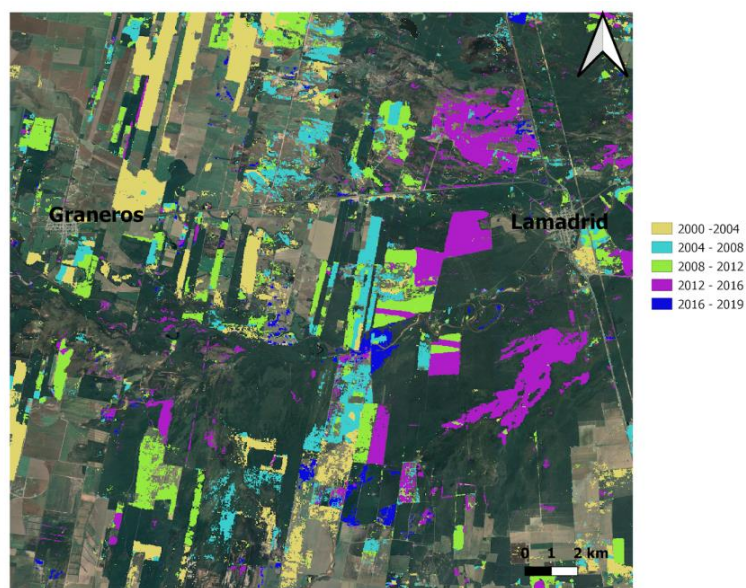


Figure 5. Forest loss map between Graneros and Lamadrid, from 2000 to 2019, Tucuman. True color zones represent non-altered regions (for the baseline), and zones with yellow, blue, pink, skyblue and green colors represent deforested area (for the hotspots).

Sampling scheme for the baseline and hotspots

Regarding the selection of monitoring points, the four most relevant criteria were selected (accessibility, ground level, distance from floodable zones, anthropic alteration) with their respective ponderation, in order to analyze 5 possible sampling points through the use of a decision matrix. **Figure 6** shows the sites which were ranked in accordance with their aptitudes. The Score is computed by adding the following: ground level (1 to 5), distance to floodable zones (1 to 5), accessibility (1 to 3), and anthropic alteration (from 1 to 3). The points with the highest scores (3 or 5 respectively) are considered as the best option, and 1 as the worst condition in every aspect. Then, the Score of every ubication is multiplied with the ponderation, and the total score provides the valorization of each point (see **Table 1**).

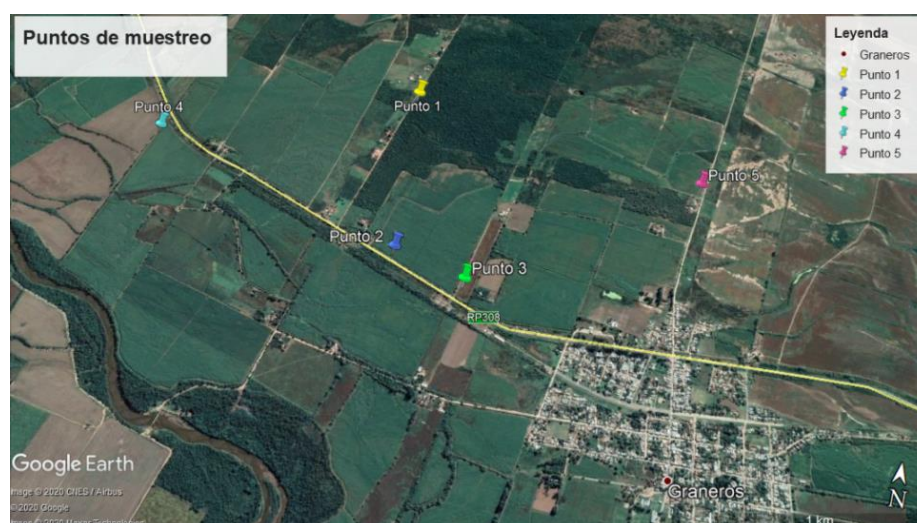


Figure 6. Map of the study area with the ubication of the selected points as baseline to a following sampling.

For the baseline sampling, the points indicate the locations where the samples were taken, given with about 50-m accuracy. As an improvement proposal, the use of SAOCOM images is considered.

However, the realized investigation in the present context offers the optimal sampling options. In order to analyze flooding zones and principal anthropogenic activities, the following hotspots were chosen (Tables 2 & 3).

Table 1. Weighing Matrix determined

Weighing		P1	P2	P3	P4	P5	
Accessibility	3	Valuation	3	5	5	2	2
		Results	9	15	15	6	6
Level	5	Valuation	5	3	3	5	2
		Results	25	15	15	25	10
Distance	5	Valuation	5	5	5	3	5
		Results	25	25	25	25	25
Anthropic alterations	3	Valuation	5	3	3	3	3
		Results	15	9	9	9	9
Totals			74	64	64	65	50

Table 2. Geographical coordinates of the sampling points for the baseline

Legend	Latitude	Longitude	Estimation
1	27° 37' 50.66" S	65° 27' 24.82" W	74
2	27° 38' 27.29" S	65° 27' 20.94" W	64
3	27° 38' 31.54" S	65° 27' 5.79" W	64
4	27° 38' 8.06" S	65° 28' 18.78" W	55
5	27° 38' 3.56" S	65° 26' 21.09" W	50

Table 3. Geographical coordinates for the hotspots determination

Hot points	Geographical positions	
1	27°38'48.48"S	65°14'26.49"W
2	27°38'49.56"S	65°14'28.10"W
3	27°39'53.21"S	65°15'54.48"W
4	27°39'55.00"S	65°15'56.21"W
5	27°40'28.91"S	65°16'44.79"W
6	27°40'30.59"S	65°16'39.95"W
7	27°40'30.86"S	65°16'44.20"W
8	27°40'50.58"S	65°18'14.98"W
9	27°40'51.87"S	65°18'16.67"W
10	27°41'17.77"S	65°19'35.15"W
11	27°41'18.54"S	65°19'40.67"W
12	27°41'21.99"S	65°19'44.17"W
13	27°41'23.85"S	65°19'49.13"W
14	27°41'26.03"S	65°19'50.95"W
15	27°40'7.10"S	65°26'37.93"W
16	27°39'56.92"S	65°26'51.65"W
17	27°37'11.66"S	65°34'38.86"W
18	27°37'13.09"S	65°34'49.85"W
19	27°38'6.12"S	65°39'19.62"W
20	27°40'38.35"S	65°47'8.82"W
21	27°40'33.03"S	65°47'12.73"W
22	27°20'47.36"S	65°37'37.62"W

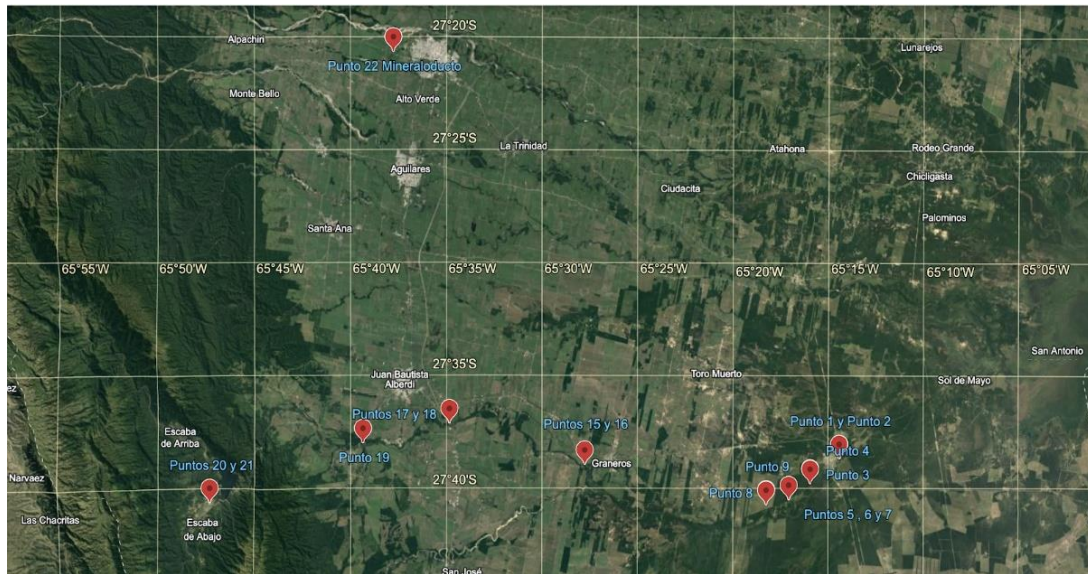


Figure 7. Map of the study area with the locations of the selected points as hotspots

3.2 – ICP Measurements

Three samples for each geographical point were obtained and measured. Each measure represents an average over the depths, absolute compositions were determined without elemental speciation (chemical form).

3.2.1– Compositional determinations for the baseline

The baseline compositional characterization for heavy metals by ICP technique after made a sampling strategy by using satellite imagery (Table 4). These showed a background concentration level of non-anthropogenic origin like pedogenesis process. High concentration levels were founded, biggest than maximum contaminant standard admitted levels (Fernandez Ochoa *et al.*, 2022).

Table 4. Concentrations of heavy metals determined on the baseline

Samples location	As[ug/g]	Cd[ug/g]	Zn[ug/g]	Cu[ug/g]	Cr[ug/g]	Hg[ug/g]	Ni[ug/g]	Pb[ug/g]
1-2 baseline	<20	<10	73±7	19±2	28±3	<29	64±3	63±6

3.1.2.2 Potentially affected zones –Compositional determination for the hotspots

Compositional analyzed elements by ICP-MS techniques from the hotspots of flooding zones, mining and sugar cane industries. The comparison between the concentration values of the baseline and the concentration values obtained from the hotspots give the Cu, Zn and Cr as contaminants in reference to some international standards as Canadian Environmental Quality Guideline (CEQG) (Fernandez Ochoa *et al.*, 2022). There were found elevated values in some geographical positions, particularly points 3-4, 6-7, 8-9 and 22. Figure 8, Figure 9 and Figure 10 show these points. Additionally, Ref. (Fernandez Ochoa *et al.*, 2022) presents an analysis for some similar soils in the region and maximum and minimum values from international conventions. However, there are different standards and for some of them the concentration values found are in a normal range.

Table 5. Concentrations of heavy metals determined on the hotpoints

Samples	As[$\mu\text{g/g}$]	Cd[$\mu\text{g/g}$]	Zn[$\mu\text{g/g}$]	Cu[$\mu\text{g/g}$]	Cr[$\mu\text{g/g}$]	Hg[$\mu\text{g/g}$]	Ni[$\mu\text{g/g}$]	Pb[$\mu\text{g/g}$]
1-2	<20	<0.2	90 \pm 9	23 \pm 2	53 \pm 5	<1	26 \pm 3	27 \pm 3
3	<20	0.29 \pm 0.03	140 \pm 10	45 \pm 4	70 \pm 7	<1	35 \pm 4	39 \pm 4
4	<20	0.29 \pm 0.03	140 \pm 10	45 \pm 4	70 \pm 7	<1	35 \pm 4	39 \pm 4
5	<20	<0.2	95 \pm 10	29 \pm 3	49 \pm 5	<1	27 \pm 3	27 \pm 3
6	<20	0.26 \pm 0.03	140 \pm 10	71 \pm 7	68 \pm 7	<1	40 \pm 4	37 \pm 4
7	<20	0.26 \pm 0.03	140 \pm 10	71 \pm 7	68 \pm 7	<1	40 \pm 4	37 \pm 4
8	<20	<0.2	110 \pm 10	38 \pm 4	69 \pm 7	<1	28 \pm 3	28 \pm 3
9	<20	<0.2	110 \pm 10	38 \pm 4	69 \pm 7	<1	28 \pm 3	28 \pm 3
12	<20	<0.2	110 \pm 10	55 \pm 5	65 \pm 7	<1	19 \pm 2	27 \pm 3
15-16	<20	<0.2	22 \pm 2	5.5 \pm 0.6	15 \pm 2	<1	7.4 \pm 0.7	20 \pm 2
17-18	<20	<0.2	75 \pm 8	20 \pm 2	40 \pm 4	<1	20 \pm 2	26 \pm 3
22A	<20	<0.2	140 \pm 10	35 \pm 0.4	56 \pm 6	<1	29 \pm 3	53 \pm 5
22B	<20	0.27 \pm 0.03	150 \pm 10	42 \pm 4	54 \pm 5	<1	29 \pm 3	39 \pm 4

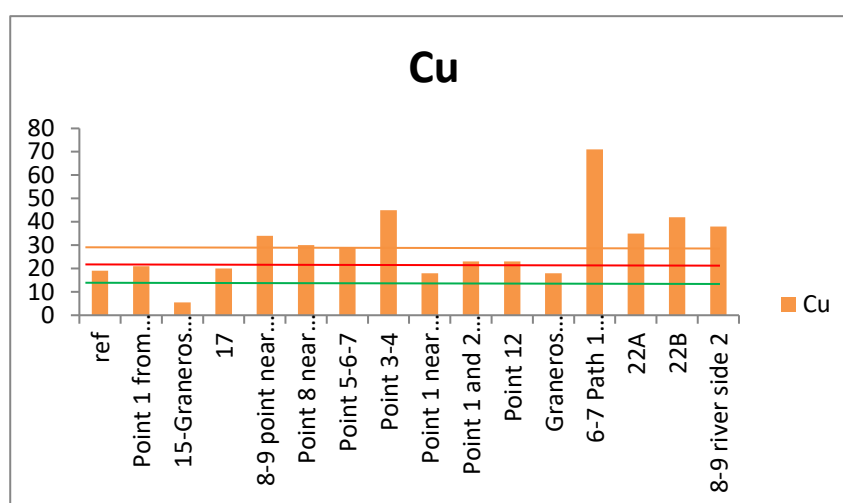


Figure 8–Total Cu concentrations (ug/g) determined by ICP at different hotpoints. Maximum and minimum values on similar soils from (Fernandez Ochoa *et al.*, 2022). Orange line level for our reference (this work)

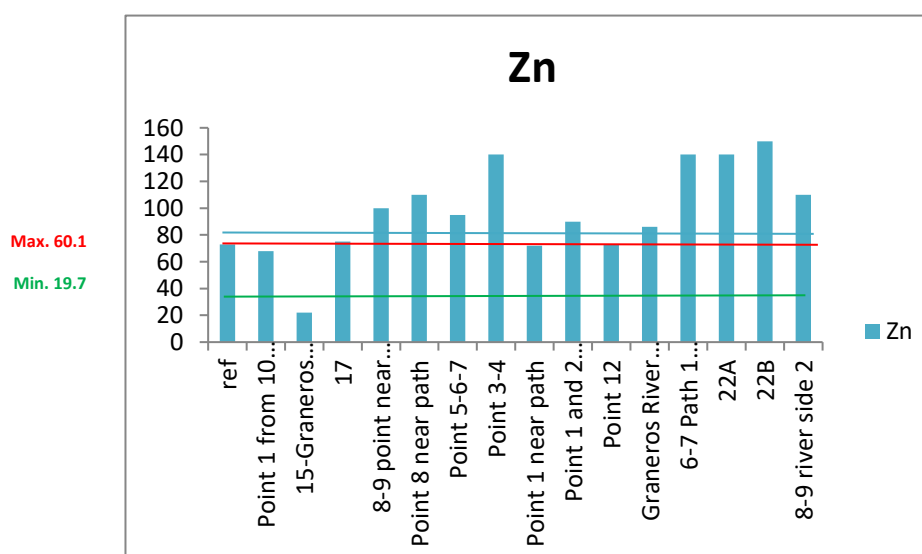


Figure 9– Total Zn concentrations (ug/g) determined by ICP at different hotpoints. Maximum and minimum values on similar soils from (Fernandez Ochoa *et al.*, 2022). Blue line level for our reference (this work)

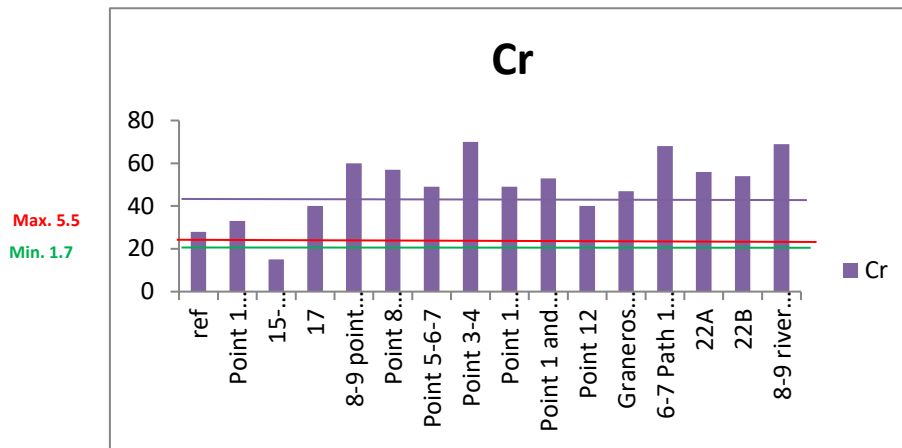


Figure 10 – Total Cr concentrations (ug/g) determined by ICP at different hotspots. Maximum and minimum values on similar soils from (Fernandez Ochoa *et al.*, 2022). Violet line level for our reference (this work)

Near to the river bends, it is possible to find high concentration levels of Cu, Cr and Zn, point 3-4, 6-7 and 8-9 (Figure 11). That suggest the retention of heavy metals on sediments by the change of flow direction.

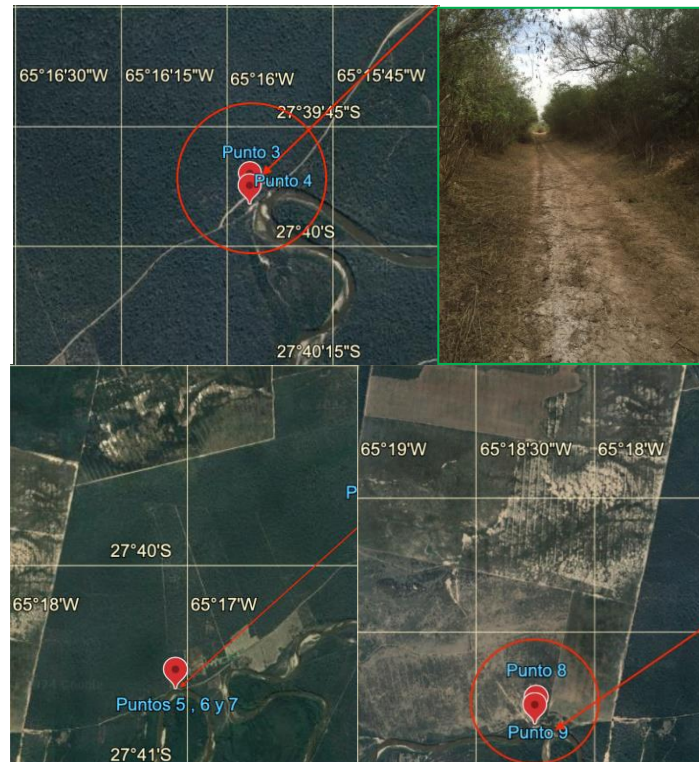


Figure 11 – Hot points located on riverbends

The point number 22 it is near to a slurry pipeline. High concentration levels at this point suggest some probably material loss, similar to reported in Alumbra's reports (Alumbra, 2006). Alumbra is Argentina's oldest open pit mine, new interdisciplinary discussions are needed in this field with different kind of stakeholder (Murguía *et al.*, 2013).

3.3 Isocomposition determinations

The analyse of isoncentration profiles allow us to infer flow directions and then propose different possibilities of sources. The matter diffusion movement is from high level concentrations to

low level concentration, following the Fick's Laws and its concentration gradients. The matter advective movement follows the hydraulic gradient, that is the Marapa current.

To analyze a dispersive matter movement without determinate the contribution of diffusive or advective flux, we use the software surfer (Software 2022) to evaluate the different levels of concentrations and in consequence to deduce concentration gradient and matter flux. This allows us to infer the possible source. Surfer software uses the typical Fick's law equations, and the results show a possible solution as a constant source as the equation (3) for the analytical concentration solution. For the case of Zn, anthropic activities seem to be more important than the advective flux from floods, with a possible source near to slurry pipeline location. For the cases of Cu and Cr, there is more than one possible source (See Figure 11, Figure 12 and Figure 13).

$$C(x, t) = C_0 \operatorname{erfc} \left(\frac{x}{\sqrt{4Dt}} \right) \quad \text{Ec. 3}$$

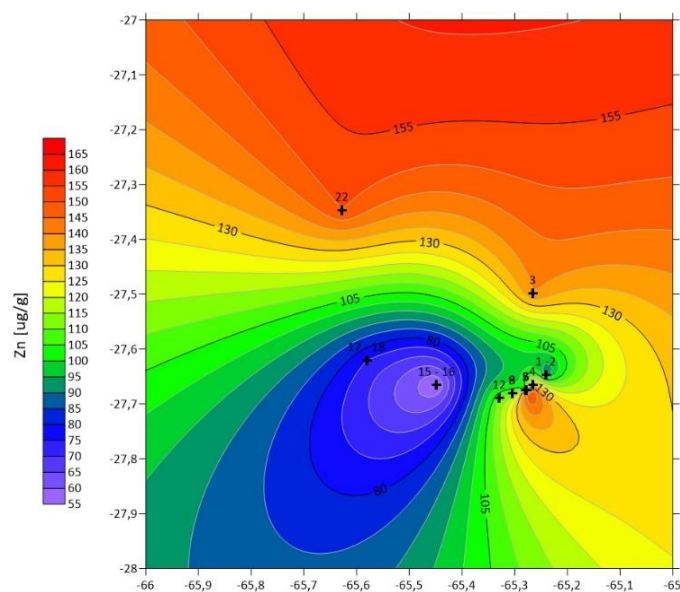


Figure 12 –Zn concentration levels (ug/g) determined by surfer (Software 222)

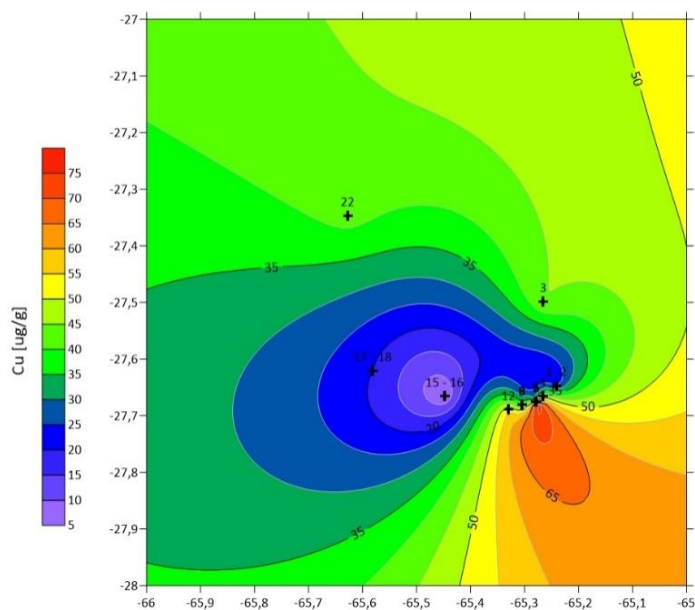


Figure 13 –Cu concentration levels (ug/g) determined by surfer (Software 222)

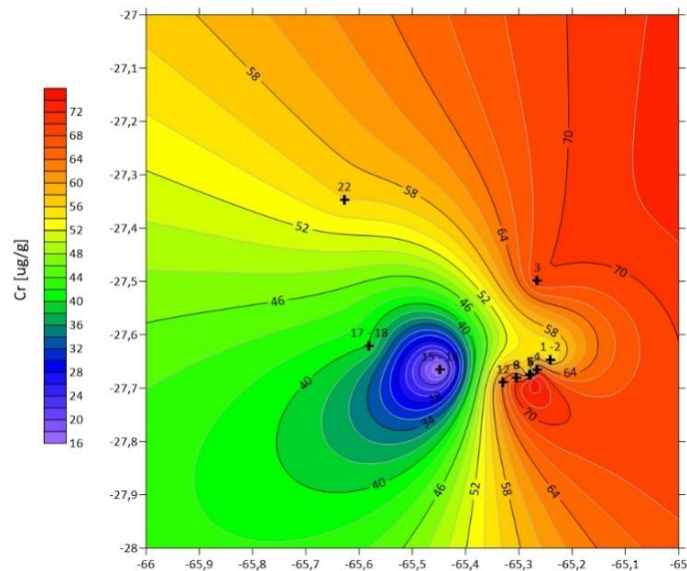


Figure 14 –Cr concentration levels (ug/g) determined by surfer (Software 222)

Different texture soils were found like shows **Figure 15**. To evaluate a new spatial direction on depth, a new study is carried out on particular hotspots to infer new possible matter movement directions.



Figure 15 –Different texture soils of hotspots

The region under study has a natural elevated level of some metals, the baseline determined shows this. The hotspot 22 suggests a diffusion process movement for some metals; instead the point 2-4,6-7 and 8-9 suggest a matter movement by advection mechanism. In this context the floods events are working in a synergy processes to disperse the matter.

The floods in the analysed region probably contribute for the redistribution of heavy metals, particularly in Lamadrid and Alberdi villages. Graneros seems to be protected by his elevation geographical level. On the other hand it is important to consider bioavailability and health risk of these contaminants. In (El Fadili *et al.*, 2024, Ferreira *et al.*, 2022) different strategies are presented using pollution indices. Normally supervision and monitoring of the contaminated area is suggested. In our case, current works to determine the elemental speciation (chemical form) are in process, then with the assessment of the pollutant characterization, the better remediation strategy could be possible.

Conclusions

The study has been able to successfully determine some matter movement directions with heavy metals. For some metals movement, the flood events seem to be not significant in this context. Therefore, a possible pollutant source is proposed.

High concentration levels of some metals were found, probably produced by a natural process in the soils, such as pedogenesis.

For a remediation program it is important to know the speciation to define the better strategy to “capture” different heavy metals found at high level concentrations.

Acknowledgement

The participation in Marapa’s Project of Matias Tabarez, Micaela Ceballos, Celeste Romero, Facundo Ortiz and Ricardo Arraga are acknowledged. The authors would like to thank Valeria Laportilla (laportilla.valeria@gmail.com) and Andrea Arganaraz (ArganarazMartinez.Andrea@gmail.com) from Tucuman Terra Organization, for their professional help in the first and second expedition campaigns. Dr. Paola Babay’s laboratory for the ICP measurements. PDS 2019 UNTREF for the funding.

CRedit authorship contribution statement. C. Corvalan Moya: Conceptualization, Management, Execution, Formal analysis, Investigation, Supervision, Writing – review & editing, Funding acquisition. C. Bruni: Investigation, Formal analysis, Writing – review & editing, A. Barbini: Investigation, Formal analysis Writing – review & editing E. Previtali: Formal analysis, Investigation, supervision, Writing – review & editing.

Disclosure statement: *Conflict of Interest:* The authors declare that there are no conflicts of interest.

Compliance with Ethical Standards: This article does not contain any studies involving human or animal subjects.

References

- Amoroso E., Castro R. G., Carlino F. J., Romero N. C., Hill R. T., and Oliver G. (1998) Screening of heavy metal-tolerant actinomycetes isolated from the Salí River. *J. Gen. Appl. Microbiol.* 44, 129–132.
- Alumbrera reports (2006): www.alumbrera.com.ar/files/informes/MAA_Sus_Report_2006_23-4-07.pdf
- Barbini A., Tabarez M., Ortiz F., Ceballos M., Lucia A., Previtali E., Corvalan-Moya C. (2021) Análisis de suelos para estudiar la seguridad socioambiental de zonas que estuvieron inundadas en la provincia de Tucumán. Determinación de la línea base. *INNOVA UNTREF. Revista Argentina De Ciencia Y Tecnología*, 1(8). <https://revistas.untref.edu.ar/index.php/innova/article/view/1239>
- Bazzi, I. El Mouaden K., Chaouay A., Ait Addi A., et al. (2020), Monitoring heavy metal contamination levels and microbiological pollution in seawater of Agadir coastal zones, *Indonesian Journal of Science & Technology* 5 (3), 463-469
- Belbachir C., Aouniti A., Khamri M., Chafi A., Hammouti B. (2013) Heavy metals (copper, zinc, iron and cadmium) in sediments and the small clam (*Chameleagallina*) of the coastal area north-east of Morocco, *J. Chem. Pharm. Res.*, 5(12), 1307-1314
- Brahimi A., Chafi A., Nouayti N., Elmsellem H., Hammouti B. (2015), Metal typology contamination of surface waters of Za River, Lower Moulouya, Eastern Morocco, *Der Pharma Chemica*, 7(9), 346-353
- Busnelli J. (2009) Evolución Histórica, Situación Actual y Perspectivas Futuras del Riesgo de Inundación en la cuenca del Río Gastona. Tucumán. Argentina. *Tesis Doctoral* de la Carrera de Posgrado en Geología (Inédita). Facultad de Ciencias Naturales e Instituto Miguel Lillo. Universidad Nacional de Tucumán. 629 p.
- Bustamante J., Díaz Delgado R., & Aragonés D. (2005) Determinación de las características de masas de aguassomeras en las marismas de Doñana mediante teledetección. *455XI Congreso Nacional de Teledetección*, 21-23 septiembre 2005. Puerto de la Cruz. Tenerife.

- Butí C., Cancino F., Ferullo S., Gamundi C. (2015) Diversity and toxicological evaluation of fish as contamination indicators for mercury, lead, cadmium, copper and arsenic in Tucumán province, Argentina., *Serie Conservación de la Naturaleza* No. 20 pp. 34.
- Díaz Gómez A. R., Gaspari F.J. (2017) Transformación territorial: Intensificación agraria y pérdida del suelo en la cuenca del río Marapa, Tucumán, Argentina, *Revista de la Facultad de Agronomía, UNLP La Plata*, 116 (2), 161-170
- El Fadili H., Ben Ali M., Rahman Md Naimur, ElMahi M., El Mostapha L., Louki Sami, (2004), Bioavailability and health risk of pollutants around a controlled landfill in Morocco: Synergistic effects of landfilling and intensive agriculture, *Heliyon* 10 (2024) e23729.
- Fernandez Ochoa B.H., Contreras E. M. and Huanchi Mamani L.E. (2022) Level of soil contamination with arsenic and heavy metals in Tiquillaca (Peru), *Revista de Investigaciones Alto andinas– Journal of High Andean Research* 24(2), 131-138, abril-junio 2022
- Ferreira S., Da Silva Junior J., Ferreira dos Santos I., M.C. de Oliveira O., Cerda V., Queiroz A. (2022) Use of pollution indices and ecological risk in the assessment of contamination from chemical elements in soils and sediments – Practical aspects, *Trend in Environmental Analytical Chemistry*, Volume 35, September 2022, e00169
- Hussin Y.A. (1995) Effect of polarization and incidence angle on radar return from urban features using L-band aircraft radar data. 10-14 July 1995. *Paper Presented at the International Geoscience and Remote Sensing Symposium, IGARSS. Quantitative Remote Sensing for Science and Applications.*
- Informe Técnico de la Comisión para el Tratamiento de la problemática de las inundaciones en el sur de la provincia de Tucumán, Catamarca y Río Hondo, (2017)
https://www.recursoshidricos.gov.ar/webdrh/_docs/CIST-Informe%20Completo.pdf
- Jalili Pirani, F., & Najafi, M. R. (2020). Recent trends in individual and multivariate compound flood drivers in Canada's coasts. *Water Resources Research*, 56, e2020WR027785. <https://doi.org/10.1029/2020WR027785>
- Jodeh S., Odeh R., Sawalhi M., Abu Obeid A., et al. (2015), Adsorption of lead and zinc from used lubricant oil using agricultural soil: equilibrium, kinetic and thermodynamic studies, *J. Mater. Environ. Sci.* 6(2), 580-591
- Owusu E., Shalaby R., Eboreime E., Nkire N., Lawal M.A., Agyapong B., Pazderka H., Obuobi-Donkor G., Adu M.K., Mao W., Oluwasina F and Agyapong V.I.O. (2022) Prevalence and Determinants of Generalized Anxiety Disorder Symptoms in Residents of Fort McMurray 12 Months Following the 2020 Flooding. *Front. Psychiatry* 13, 844907. doi: 10.3389/fpsyt.2022.844907
- Leckie D.G., Ranson K. (1998) Forestry applications using imaging radar. *Principles and Applications of Imaging Radar* 2. pp. 435–509
- Liao H.-Y., & Wen T.-H. (2020) Extracting urban water bodies from high-resolution radar images: Measuring the urban surface morphology to control for radar's double bounce effect. *International Journal of Applied Earth Observation and Geoinformation*, 85, 102003. doi:10.1016/j.jag.2019.102003
- Mazraeh N., Khorodamini S., Hesam A., Rasti A., Khodarahmi S.M., Aganj N., and Sheikhi S. (2023) The Role of Social Interest and Empathy on Helping Behaviors during Floods, *Anales de psicología / annals of psychology*, 39, n° 1 (January), 119-126, <https://doi.org/10.6018/analesps.515131>
- McFeeters K. (1996) The use of the Normalized Difference Water Index (NDWI) in the delineation of open water features, *International Journal of Remote Sensing*, 17:7, 1425-1432,
- Murguía D.I. and Böhlting K. (2013) Sustainability reporting on large-scale mining conflicts: the case of Bajo de la Alumbrera, Argentina, *Journal of Cleaner Production*, 41, February 2013, Pages 202-209
- Nyiramigisha P., Komariah and Sajidan (2021) *Reviews in Agricultural Science*, 9, 271–282, https://dx.doi.org/10.7831/ras.9.0_271
- Recavarren P., (2016) La producción agropecuaria en Olavarría, Benito Juárez, Laprida y Gral. La Madrid: evolución y desafíos a futuro, in: *INTA, E. (Ed.)*, p. 143.

- Roessner S., Segl K., Bochow M., Heiden U., Heldens W., Kaufmann H. (2011) Potential of hyperspectral remote sensing for analyzing the urban environment. - In: Yang, X. (Ed.), *Urban remote sensing: monitoring, synthesis and modelling in the urban environment*, Wiley-Blackwell, 49-62.
Software: <https://www.goldensoftware.com/products/surfer/>
- Yan, X.; Liu, M.; Zhong, J.; Guo, J.; Wu, W. (2018) How Human Activities Affect Heavy Metal Contamination of Soil and Sediment in a Long-Term Reclaimed Area of the Liaohe River Delta, North China. *Sustainability*, 10, 338. <https://doi.org/10.3390/su10020338>
- Villegas L. B. and Figueroa L. I. C. (2002) Communities of yeasts tolerant to heavy metals from different polluted sites of Argentina. *102nd General Meeting of the American Society for Microbiology*. Salt Palace Convention Center, Salt Lake City, Utah, May 19–23 (2002).
- Xu Hanqiu (2006), Modification of normalised difference water index (NDWI) to enhance open water features in remotely sensed imagery, *International Journal of Remote Sensing*, 27:14, 30253033, DOI: [10.1080/01431160600589179](https://doi.org/10.1080/01431160600589179)

(2024): <http://www.jmaterenvirosci.com>